Analysis of g-r Noise Upconversion in Oscillators

T. Felgentreff[1], W. Anzill[1], G. Olbrich[1], P. Russer[1,2]

[1] Technische Universität München, Lehrstuhl für Hochfrequenztechnik
Arcisstraße 21, 80290 München, Germany
[2] Ferdinand-Braun-Institut für Höchstfrequenztechnik
Rudower Chaussee 5, 12489 Berlin, Germany

Abstract

In this paper the upconversion of g-r noise to oscillator phase noise is analysed for the first time. The treatment of g-r noise sources showing a Lorentzian spectrum is implemented in a time domain noise calculation program using the perturbation method. Measurements and simulations show that the upconverted g-r noise dominates the phase noise characteristics of AlGaAs/GaAs–HEMT oscillators in the frequency range between 10 kHz and 8 MHz besides the carrier.

Introduction

The simulation of oscillator noise in time domain uses a perturbation ansatz [1]. Within this approach it is possible to include white noise and $f^{-\alpha}$ noise sources into the calculation of the oscillator's phase noise. Especially III/V–devices containing layers with Al show strong g-r noise superimposed to the fundamental $f^{-\alpha}$ noise (Fig. 2 and [2, 3]). This additional g-r noise results from deep level traps located in the AlGaAs-layer and shows strong bias dependence [4, 5]. It dominates the noise behavior of the active element at frequencies about 100 kHz. Measured phase noise data of HEMT oscillators show that the upconverted g-r noise degrades the phase noise performance in this frequency range [6, 7].

In this paper we present a method for the treatment of g-r noise showing a Lorentzian spectrum. The g-r noise is included into the time domain phase noise simulation (TDPNS) method introduced by Kärtner [1]. In the second part of the paper the method is applied to a HEMT oscillator. The result demonstrates the influence of g-r noise to the phase noise of oscillators, and the calculated data agree with the measured results within the measurement accuracy of ±2 dB.

Theoretical Approach

For the application of the TDPNS method, the oscillator circuit is approximated by a lumped element circuit model. The Langevin equations, a set of ordinary first order nonlinear differential equations, describe the deterministic and stochastic behavior of the oscillator.

$$\dot{\boldsymbol{x}} = f(\boldsymbol{x}, \boldsymbol{\xi}, y, z) \quad (1)$$

$$\boldsymbol{x} \in I\!R^N,\ \boldsymbol{\xi} \in I\!R^K,\ y \in I\!R,\ z \in I\!R.$$

The components of the vector $\boldsymbol{x}$ are the state variables. The variables $\boldsymbol{\xi}$, y and z describe the white, the $f^{-\alpha}$ and the g-r noise sources. Since the amplitudes of the noise sources can be considered to be very small compared with the amplitudes of the unpertubated state variables, it is sufficient to take it into account up to the first order term only.

$$\dot{\boldsymbol{x}} = f(\boldsymbol{x}) + \mathbf{G}(\boldsymbol{x})\,\boldsymbol{\xi} + \boldsymbol{g}(\boldsymbol{x})\,y + \boldsymbol{r}(\boldsymbol{x})\,z = f(\boldsymbol{x}) + \zeta(\boldsymbol{x}) \quad (2)$$

The state vector $\boldsymbol{x}^0(t)$ describing the oscillator's steady state is calculated by neglecting the contributions of the noise sources. The noise sources cause a deviation from the unperturbed limit cycle. This deviation is separated into a tangential and a transversal part. The first one causes a time shift $\vartheta(t)$ leading to the phase noise of oscillators.

$$\boldsymbol{x}(t) = \boldsymbol{x}^0(t + \vartheta(t)) + \boldsymbol{\Delta}\mathbf{x}(t + \vartheta(t)) \quad (3)$$

Substituting $s = t + \vartheta(t)$ and requesting only small deviations leads to

$$\boldsymbol{x}'(s)\vartheta'(t) + \boldsymbol{\Delta}\mathbf{x}'(s) = \mathbf{DF}_{ij}(\boldsymbol{x}^0(s))\boldsymbol{\Delta}\mathbf{x}(s) + \zeta(\boldsymbol{x}^0(s)). \quad (4)$$

WE 4C

The elements of the Jacobian $\mathbf{DF}_{ij}(\boldsymbol{x}^0(s))$ define a linear time periodical differential equation for a small deviation $\mathbf{\Delta x}$ from the upertubed steady state. Restricting the solution of this equation to the relevant solution of the phase process of the system, we obtain

$$\dot{\vartheta}(t) = \boldsymbol{v}_1^T(s)\boldsymbol{\zeta}(\boldsymbol{x}^0(s)). \tag{5}$$

The solution $\vartheta(t)$ for the white noise sources ξ and $f^{-\alpha}$ noise sources y has already been published by Kärtner [1]. In this paper we concentrate on the treatment of the g-r noise sources showing the Lorentzian spectrum

$$C^z(f) = \frac{\alpha_{gr}}{1 + (f\,\tau_{gr})^2} \quad . \tag{6}$$

The term α_{gr} and the time constant of the trap level τ_{gr} are determined from low frequency noise measurements. The term $\boldsymbol{r}(x)z$ in eq. (2) describes the influence of the g-r noise sources on the state variables. The integration of eq. (5) using $\varphi(t) = \omega_0\vartheta(t)$ yields

$$\varphi(t) = \omega_0 \int_0^t \boldsymbol{v}_1^T(s)\boldsymbol{r}(\boldsymbol{x}^0(s))z(s))ds. \tag{7}$$

Using a fourier series representation for the periodic function $r_1(s) = \boldsymbol{v}_1^T\,\boldsymbol{r}(\boldsymbol{x}^0(s))$ gives

$$\varphi(t) = \omega_0 \int_0^t \sum_{l=-\infty}^{+\infty} (\hat{r}_{1,l}\, e^{jl\omega_0 s})z(s)ds. \tag{8}$$

Because the major amount of the integral results from the term $l = 0$, the term $r_1(s)$ can be replaced by the mean value $r_{1,0}$ of a period [1]. This yields

$$\varphi(t) = \omega_0\, r_{1,0} \int_0^t z(s)ds. \tag{9}$$

Calculating the correlation function $c_{\Delta\dot{\varphi}}(\tau)$ of the phase derivative $\Delta\dot{\varphi}(\tau)$ results in

$$c_{\Delta\dot{\varphi}}(\tau) = |A|^2 < \dot{\varphi}(t+\tau)\,\dot{\varphi}(t) >= |A|^2\,\omega_0^2\,|r_{1,0}|^2\,c^z(\tau). \tag{10}$$

In this equation A describes the fourier coefficients of the state variables. The transformation into the frequency domain results in

$$C_{\Delta\dot{\varphi}}(f) = |A|^2\omega_0^2\,|r_{1,0}|^2\,C^z(f). \tag{11}$$

By integrating the phase variations and replacing C^z by (6) the correlation spectra of the phase fluctuations due to the g-r noise sources can be calculated

$$C_{\Delta\varphi}(f) = |A|^2\frac{\omega_0^2}{\omega^2}|r_{1,0}|^2\frac{\alpha_{gr}}{1 + (f\,\tau_{gr})^2}. \tag{12}$$

As a result the g-r noise sources produce a phase noise spectrum given by the third term in eq. (13). The first and second term result from the white and the $f^{-\alpha}$ noise sources of the circuit [1]. Therefore $\mathcal{L}(f_m)$ describes the phase noise spectrum caused by all noise sources.

$$\mathcal{L}(f_m) = \frac{\Delta f_{3dB}}{\pi\, {f_m}^2} + \sum_{k=1}^{K}|g_{1,0}^k|\frac{\omega_0^2\,c_k}{|2\pi\, f_m|^{2+\alpha}} + \sum_{i=1}^{I}|r_{1,0}^i|^2\frac{\omega_0^2}{|2\pi\, f_m|^2}\frac{\alpha_{gr}}{1 + (f_m\,\tau_{gr})^2} \tag{13}$$

The phase noise caused by the g-r noise sources decreases with 20 dB per frequency decade for $f_m \ll 1/\tau_{gr}$, which is the same frequency dependency as for the white noise sources. For frequencies $f_m \gg 1/\tau_{gr}$ the phase noise due to the g-r noise decreases with 40 dB per frequency decade. The term $|r_{1,0}^i|^2$ is computed using the network equations and it describes the mixing behavior of the g-r noise to the noise sidebands of the carrier.

Modeling of the HEMT device

Figure 1 shows the large signal and noise equivalent circuit we use for the intrinsic HEMT device, including the parasitic resistive elements.

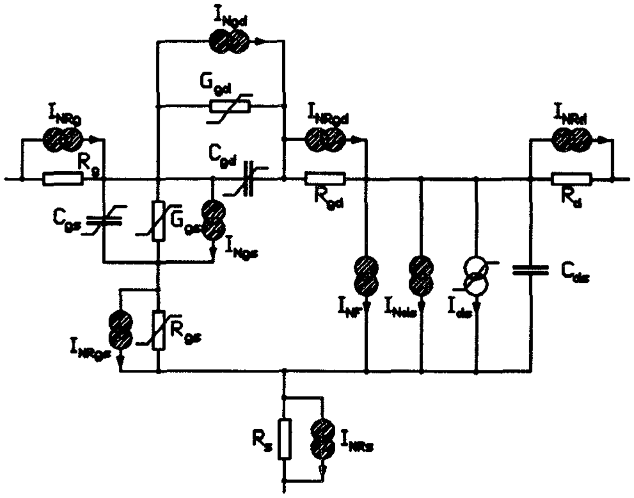

Figure 1: Large signal and noise equivalent circuit of the intrinsic HEMT

The signal properties of the HEMT were modeled using the nonlinear data based model presented in [9]. The high frequency noise performance of the HEMT is described by the model given in [10, 11], which uses three uncorrelated white noise current sources ($I_{Nds}, I_{NRgs}, I_{NRgd}$) associated with the resistive elements of the intrinsic transistor. The parameters of these noise sources are determined from noise parameter measurements.

Baseband noise measurements on HEMT devices were carried out to determine the bias dependent low frequency noise spectra. The measured noise spectra (Fig. 2) show fundamental $f^{-\alpha}$ and superimposed g-r noise.

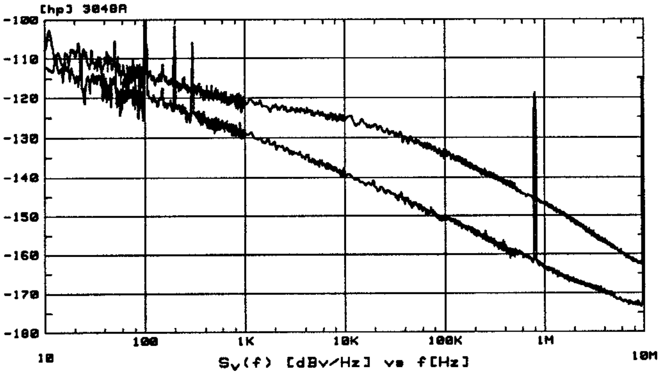

Figure 2: Measured baseband noise of an AlGaAs/GaAs-HEMT showing $f^{-\alpha}$ and additional g-r noise at $V_{ds} = 1.0$ V and $V_{gs} = -1.1$ V, $I_{ds} = 1.8$ mA; $V_{gs} = -0.5$ V, $I_{ds} = 26.3$ mA

The low frequency noise is modeled as a noise current source I_{NF} in the channel of the HEMT. The noise source I_{NF} includes the g-r noise source showing a Lorentzian spectrum and the fundamental $f^{-\alpha}$ noise source showing a spectrum proportional to $f^{-\alpha}$. The bias dependency of the $f^{-\alpha}$ noise current source is described by the empirical model presented in [6].

To demonstrate the effect of the g-r noise source to the phase noise $\mathcal{L}(f_m)$ of the oscillator, we use a Lorentzian spectrum with $\tau_{gr} = 5\mu s$, which is equivalent to a corner frequency $f_c = 200$ kHz of the Lorentzian spectrum. As a first order approximation the amplitude of the g-r noise current source In_{gr} was determined to be linearly dependent on the bias channel current $In_{gr} = \gamma I_{ds}$ (Fig. 3).

Oscillator Example

As an example we applied the noise calculation to a HEMT oscillator at 15.2 GHz. The oscillator uses an AlGaAs/GaAs-HEMT as the active device. The circuit is build up with coplanar lines to easily realize short circuits [8] and was hybrid integrated on an Al_2O_3-substrate. The layout of the oscillator is shown in Fig. 4. The coplanar resonator at the left is coupled to the gate of the HEMT device through a coupling slot in the coplanar line.

A comparison of measured and calculated phase noise is given in Fig. 5. Up to frequencies $f_m < 10$ kHz the $f^{-\alpha}$ noise determines the phase noise of the oscillator. At frequencies between 10 kHz and 8 MHz, the g-r noise determines the phase noise performance. The white noise sources dominate the phase noise at frequencies above 8 MHz. Because the DX-centers consist of more than one deep level trap there should be considered more than one g-r noise source to model the low frequency noise of the HEMT device more exactly. Using several g-r noise sources the calculated phase noise result would show in a wider frequency range increased phase noise, which would match more precisely the measured phase noise performance.

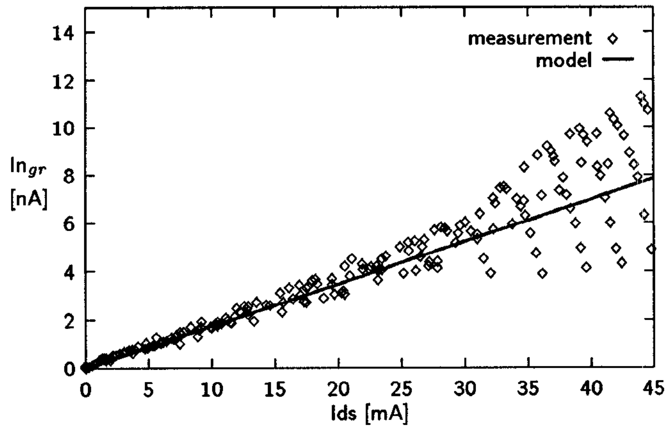

Figure 3: Measured and modeled g-r noise current source of an AlGaAs/GaAs-HEMT

Conclusion

In this paper we present a method for the treatment of g-r noise showing a Lorentzian spectrum. The g-r noise sources are included in the phase noise simulation method given by Kärtner [1]. Using this calculation method it is now possible to do oscillator phase noise calculations in the time domain considering all

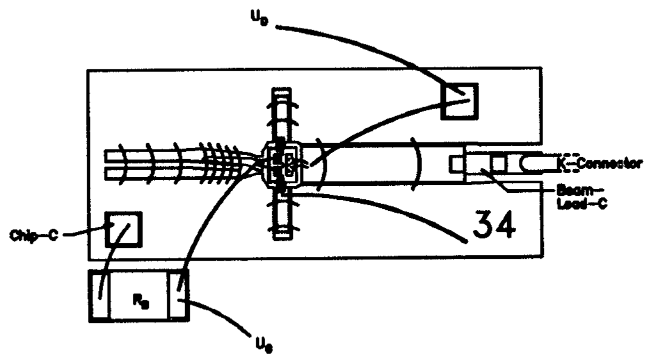

Figure 4: Layout of the hybrid integrated coplanar HEMT oscillator

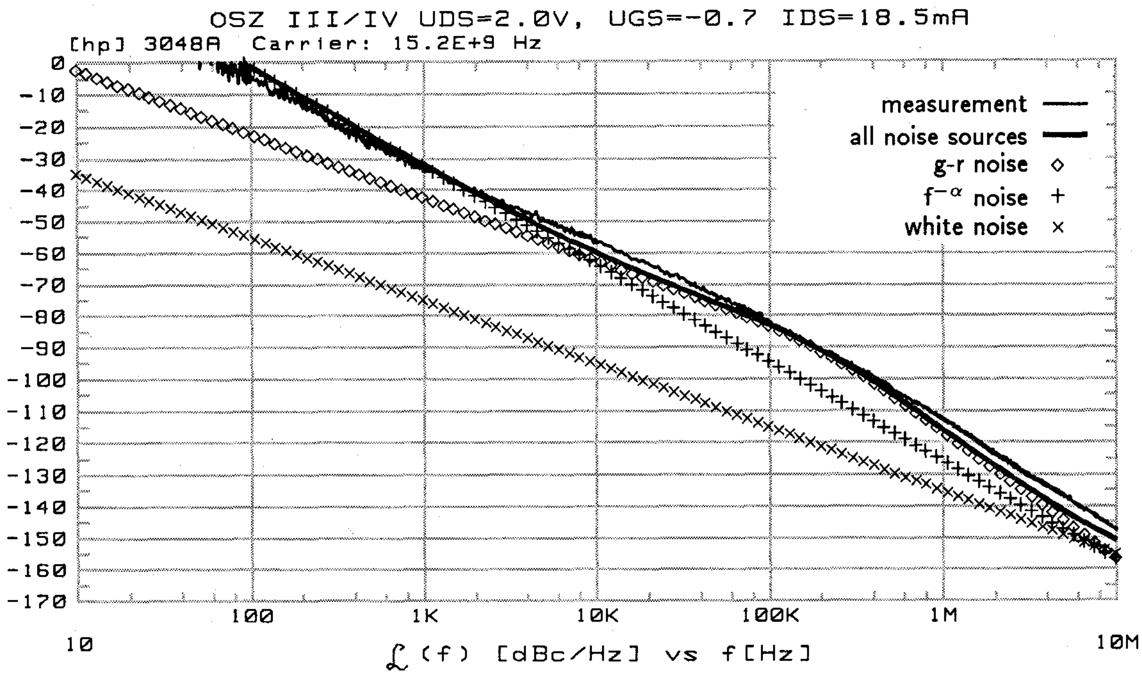

Figure 5: Measured and calculated phase noise performance of the coplanar HEMT oscillator

important low frequency noise contributions. We applied this method to a HEMT oscillator. The results show that upconverted g-r noise determines the phase noise performance of AlGaAs/GaAs-HEMT oscillators in the frequency range from 10 kHz to 8 MHz besides the carrier.

Acknowledgement

This research project has been financially supported by the Deutsche Forschungsgemeinschaft (SFB 348).

References

[1] F. X. Kärtner: *Analysis of white and $f^{-\alpha}$ noise in oscillators*, International Journal of Circuit Theory and Application, Vol. 18, pp. 485–519, 1990.

[2] S. M. Lui, M. B. Das, W. Kopp, H. Morkoç: *Noise Behavior of 1-μm Gate-Length Modulation-Doped FET's From* 10^{-2} to 10^8 Hz, IEEE Electron Device Letters, Vol. 6, No. 9, Sep. 1985, pp. 453–455.

[3] G.R. Olbrich, T. Schenk: *Measurement of 1/f-noise on microwave transistors*, ISSSE 1992 Int. Symposium on Signals, Systems and Electronics, Paris, Sept. 1–4, 1992, S. 772–775.

[4] S. Kugler: *Generation-Recombination Noise in the Saturation Regime of MODFET Structures*, IEEE Trans. on Electron Devices, Vol. 35, No. 5, May 1988, pp. 623–628.

[5] R. Plana, L. Escotte, O. Llopis, H. Amine, T. Parra, M. Gayral, J. Graffeuil: *Noise in AlGaAs/InGaAs/GaAs Pseudomorphic HEMT's from 10 Hz to 18 GHz*, IEEE Trans. on Electron Devices, Vol. 40, No. 5, May 1993, pp. 852–858.

[6] G.R. Olbrich, T. Felgentreff, W. Anzill, P. Russer: *Calculation of HEMT Oscillator Phase Noise Using Large Signal Analysis in Time Domain*, IEEE MTT-S Digest 1994, pp. 965–968.

[7] O. Llopis, R. Plana, H. Amine, L. Escotte, J. Graffeuil: *Phase Noise in Cryogenic Microwave HEMT and MESFET Oscillators*, IEEE Trans. MTT, Vol. 41, No. 3, March 1993, pp. 369–374.

[8] R. A. Pucel: *Design Considerations for Monolithic Microwave Circuits*, IEEE Trans. MTT, Vol. 29, No. 6, Jun. 1984, pp. 513–534.

[9] T. Felgentreff, G. Olbrich, P. Russer: *A Smallsignal Databased HEMT Model for Nonlinear Time Domain Simulation*, SISDEP 93, Simulation of Semiconductor Devices and Processes, Vol. 5, pp. 269–172, Springer Verlag Wien.

[10] T. Felgentreff, G. Olbrich, P. Russer: *Noise Parameter Modeling of HEMTs with Resistor Temperature Noise Sources*, IEEE MTT-S Digest 1994, pp. 853–856.

[11] M. Pospieszalski: *Modeling of Noise Parameters of MESFET's and MODFET's and Their Frequency and Temperature Dependence*, IEEE Trans. MTT, Vol. 37, No. 9, Sep. 1989, pp. 1340–1350.